EARTHQUAKE ENGINEERING AND STRUCTURAL DYNAMICS
Earthquake Engng Struct. Dyn. 2000; **29**:377–396

Passive and active control of three-dimensional buildings

Yoyong Arfiadi and Muhammad N. S. Hadi*,†

Department of Civil, Mining and Environmental Engineering, University of Wollongong, NSW 2522, Australia

SUMMARY

The majority of the recent research effort on structural control considers two-dimensional plane structures. However, not all buildings can be modelled as plane structures, thus limiting the capability of the proposed procedures only to regular and symmetrical structures. A new procedure is developed in this paper to analyse three-dimensional buildings utilizing passive and active control devices. In the building model, the floors are assumed rigid in their own plane resulting in three degrees of freedom at each floor. Two types of active control devices utilizing an active tuned mass damper and an active bracing system are considered. The effect of passive mass dampers and active control force in the equations of motion is incorporated by using the Hamilton's principle. The passive parameters of the dampers as well as the controller gain is then optimized using a genetic based optimizer where the H_2, H_∞ and L_1 norms are taken as the objective functions. Copyright © 2000 John Wiley & Sons, Ltd.

KEY WORDS: three-dimensional building, structural control; H_2 norm, H_∞ norm, L_1 norm, direct output feedback, genetic algorithm

INTRODUCTION

During the past three decades, structural control has been an attractive focus of research and has received considerable attention from researchers. The objective is to reduce the structural response, due to excessive vibration caused by earthquake and wind loads, by means of passive or active control devices or their combinations. In a passive control system, the reduction of the response can be achieved by the addition of materials or devices that can dissipate energy. Hence, passive control does not require an external energy since the energy dissipation can be activated by the passive system itself. Among passive control devices that have been applied in practice are tuned mass dampers, base isolations and viscoelastic dampers. While passive control is attractive due to its simplicity, active control is attractive due to its potential use. Since originated by Yao

* Correspondence to: Muhammad N. S. Hadi, Department of Civil, Mining and Environmental Engineering, University of Wollongong, Wollongong, NSW 2522, Australia.
† E-mail: m.hadi@uow.edu.au

Received 25 March 1999
Revised 2 September 1999
Accepted 14 September 1999

[1] active control recently has received an extensive research. By the combination of the sensor to measure the response, actuators to drive the control force, and a computer to compute an appropriate control force, the motion of the structure can be controlled by a designer. Devices that have been proposed include active tendon control [2], active tuned mass dampers [3] and active bracing systems [4]. In addition to the application of the active force to the passive system, some new devices such as electro-rheological fluid dampers [5] and magneto-rheological dampers [6], for example, recently are proposed to be applied to civil engineering structures resulting in a new class of semiactive control. In addition, the combination of active and passive control, as a hybrid control system, has also been proposed to be applied to civil engineering structures.

Despite this promising development, recent research effort regarding structural control, especially active control structures, usually consider two-dimensional plane frame structures only. Therefore, it limits the applicability of this method into simple and symmetrical structures. As buildings are three-dimensional in geometry, it is necessary to carry out the research in three dimensions rather than two dimensions. This will represent buildings in a more natural pattern and reflect its true behaviour.

Few researchers have considered three-dimensional structures as the building model. Samali *et al.* [7] studied the application of active mass damper in three-dimensional buildings. The transfer function matrix method was used to analyse the lateral and torsional responses of the buildings. Kobori *et al.* [8, 9] presented a method of controlling three-dimensional building using active mass damper as well as in Higashino and Aizawa [10] and Maebayashi *et al.* [11] without detailed discussion on structural model. Fur *et al.* [12] studied active mass dampers by utilizing the model of Kan and Chopra [13] for the building. In Loh and Lin [14] a three-dimensional building was also used as the example in their studies.

Considering the current research so far, the objectives of this paper are: (i) to develop a procedure to analyse three-dimensional structures that contains passive and active control systems, (ii) to optimize the passive devices as well as the control force by using a modern control theory. A mass damper and an active bracing system are utilized in this paper for the numerical example. The optimization of passive mass dampers systems as well as the computation of the optimal control force is performed by using a genetic based optimizer [15, 16] in which the objective functions can be H_2, H_∞ and L_1 norms. Another aspect that should be considered is that the responses of the structure should be minimized with respect to the earthquake which can be applied in the x and y direction of the structures. Note also that the feedback control system utilized in this paper falls into the family of static (direct) output feedback controller, where the output measurement can be directly multiplied by the gain obtained using the genetic-based optimizer.

THREE-DIMENSIONAL BUILDINGS WITHOUT PASSIVE AND ACTIVE DEVICES

The three-dimensional building model and analysis have been considered by some researchers [13, 17–22]. This paper utilizes the model similar to the one in Wilson *et al.* [19, 20] but with the formulation of the stiffness matrix adopted from the general element stiffness matrix of three-dimensional space frame element. The building is modelled as a structure composing of members connected by a rigid floor diaphragm such that it has three degree of freedom at each floor, i.e., lateral displacements in two perpendicular directions and a rotation with respect to a vertical

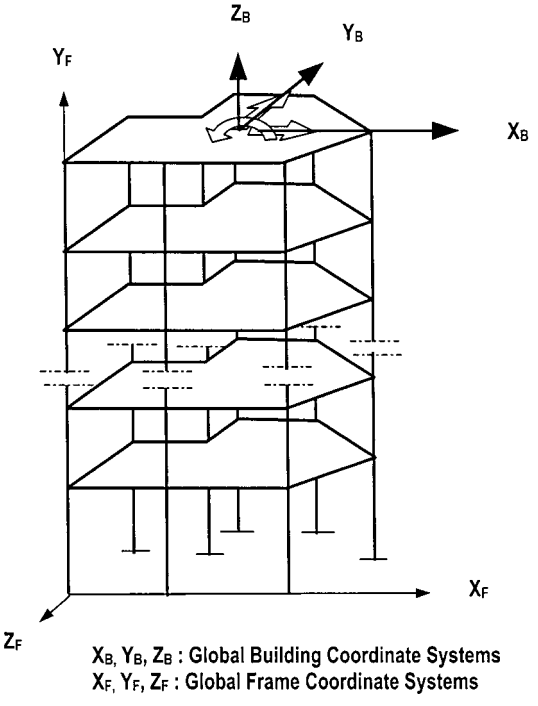

Figure 1. Three-dimensional building with rigid floor model.

axis. Two co-ordinate systems are defined as Global Frame Co-ordinate and Global Building Co-ordinate Systems, respectively, as well as another local (member) co-ordinate system. The model of the building can be seen in Figure 1.

To build the stiffness matrix in terms of Global Building Co-ordinate System, first the element stiffness matrix of each member is transformed into the Global Frame Co-ordinate System, where this coordinate system can be located anywhere. The stiffness matrix of the structure as well as the load vector with respect to the Global Frame Co-ordinate System is then assembled by the standard procedure developed in the matrix method of structural analysis. In assembling the stiffness matrix, the transformation of coordinates following a third-point convention of three-dimensional transformation [23] was adopted. As we will condense out displacements that do not relate to the rigid floor freedom, displacements of each member are assembled such that the resulting structure's stiffness matrix in terms of Global Frame Co-ordinate System has the form

$$\mathbf{K}_F \Delta_F = \mathbf{R}_F \tag{1}$$

where $\mathbf{K}_F = \sum \mathbf{K}_e$, $\mathbf{R}_F = \sum \mathbf{R}_e$, $\mathbf{K}_e$ = element stiffness matrix in the Global Frame Co-ordinate System, $\mathbf{R}_e$ = load vector in the Global Frame Co-ordinate System, Δ_F = displacement vector, and the summation is taken for all members in the structure. Equation (1) may be partitioned in the form

$$\begin{bmatrix} \mathbf{K}_{CC} & \mathbf{K}_{CR} \\ \mathbf{K}_{RC} & \mathbf{K}_{RR} \end{bmatrix} \begin{Bmatrix} \Delta_{FC} \\ \Delta_{FR} \end{Bmatrix} = \begin{Bmatrix} \mathbf{R}_{FC} \\ \mathbf{R}_{FR} \end{Bmatrix} \tag{2}$$

in which Δ_{FC} contains Z_B displacement, rotation about X_B-axis and rotation about Y_B-axis, referred to as group a displacements; Δ_{FR} contains X_B displacement, Y_B displacement and rotation about Z_B-axis, referred to as group b displacements.

Utilizing the static condensation technique, Equation (2) can be transformed such that it retains the displacements corresponding to the rigid floor displacements (group b displacements) in the form

$$\mathbf{K}^*_{RR}\Delta_{FR} = \mathbf{R}^*_{FR} \tag{3}$$

where

$$\mathbf{K}^*_{RR} = \mathbf{K}_{RR} - \mathbf{K}_{RC}\mathbf{K}^{-1}_{CC}\mathbf{K}_{CR} \tag{4}$$

$$\mathbf{R}^*_{FR} = \mathbf{R}_{FR} - \mathbf{K}_{RC}\mathbf{K}^{-1}_{CC}\mathbf{R}_{FC} \tag{5}$$

in which the first sub-matrix equation of Equation (2) of the form

$$\Delta_{FC} = \mathbf{K}^{-1}_{CC}(\mathbf{R}_{FC} - \mathbf{K}_{CR}\Delta_{FR}) \tag{6}$$

has been used to obtain Equation (3).

The stiffness matrix in terms of Global Building Co-ordinates can be determined by using a matrix transformation and following standard procedures in the matrix method. The group b displacements of joint i at floor n can be written in terms of rigid floor displacements according to

$$\begin{Bmatrix} \Delta^i_{FR1,n} \\ \Delta^i_{FR2,n} \\ \Delta^i_{FR3,n} \end{Bmatrix} = \begin{bmatrix} c_\alpha & s_\alpha & d_x \\ s_\alpha & -c_\alpha & d_z \\ 0 & 0 & 1 \end{bmatrix} \begin{Bmatrix} r_{x,n} \\ r_{y,n} \\ r_{\theta,n} \end{Bmatrix} \tag{7}$$

where $\Delta^i_{FR1,n}$, $\Delta^i_{FR2,n}$, $\Delta^i_{FR3,n}$ = displacements of joint i at floor-n in X_B- and Y_B-axis, and rotation about Z_B axis, respectively, $r_{x,n}$, $r_{y,n}$, $r_{\theta,n}$ = displacements in X_B and Y_B directions and rotation of the floor-n about Z_B axis, d_x = distance from the origin of the Global Building Co-ordinates to the line of action of x-displacement of the joint (Δ_{FR1}), d_z = distance from the Global Building Co-ordinates to the line of action of z-displacements of the joint (Δ_{FR2}), $c_\alpha = \cos\alpha$, $s_\alpha = \sin\alpha$, α = anti-clockwise angle from X-Global building co-ordinates axis to the line of action of the x-displacement of the joint (Δ_{FR1}). The values of d_x and d_z might be positive or negative depending on whether the building rotation causes positive or negative displacement to the joint. When the building rotation causes positive joint displacement then the positive value of d_x or d_z should be used. Note that usually the X-Global Frame Co-ordinate and the X-Global Building Co-ordinate System axes are in parallel (or can be made so) therefore $\alpha = 0$ so that $c_\alpha = 1$ and $s_\alpha = 0$.

Equation (7) can be written in a simple form as

$$\Delta^i_{FR,n} = \mathbf{a}^i_n\, \mathbf{X}_{3D,n} \tag{8}$$

where $\mathbf{a}^i_n$ is the transformation matrix of joint i at floor n, $\Delta^i_{FR2,n}$ = group b displacements for joint i at floor n and $\mathbf{X}_{3D,n}$ = building displacement at floor n.

By summing up for all joints at floor n the transformation of displacements can be written as

$$\Delta_{FR,n} = \mathbf{a}_n\mathbf{X}_{3D,n} \tag{9}$$

where $\Delta_{FR,n}$ = group b displacements for all joints at floor n, $\mathbf{a}_n$ = transformation matrix for joint at floor n and $\mathbf{X}_{3D,n}$ = building displacement at floor n. In Equation (9), $\Delta_{FR,n}$, $\mathbf{a}_n$ and $\mathbf{X}_{3D,n}$ contain elements as follows:

$$\Delta_{FR,n} = \begin{Bmatrix} \Delta^1_{FR,n} \\ \Delta^2_{FR2,n} \\ \vdots \\ \Delta^{NJn}_{FR,n} \end{Bmatrix}_{3NJn\times 1}, \qquad \mathbf{a}_n = \begin{bmatrix} \mathbf{a}^1_n \\ \mathbf{a}^2_n \\ \vdots \\ \mathbf{a}^{NJn}_n \end{bmatrix}_{3NJn\times 3}, \qquad \mathbf{X}_{3D,n} = \begin{Bmatrix} r_{x,n} \\ r_{y,n} \\ r_{\theta,n} \end{Bmatrix}_{3NJn\times 1} \tag{10a–c}$$

where NJn = the total number of joints at floor n. Considering the transformation of joints at floor n in Equations (9) and (10), the relation of group b displacements to the building displacement can be written as

$$\Delta_{FR} = \mathbf{a}\mathbf{X}_{3D} \tag{11}$$

where

$$\Delta_{FR} = \begin{Bmatrix} \Delta_{FR,1} \\ \Delta_{FR,2} \\ \vdots \\ \Delta_{FR,NF} \end{Bmatrix}_{3NTF\times 1}, \qquad \mathbf{a} = \begin{bmatrix} \mathbf{a}_1 & \mathbf{0} & \cdots & \mathbf{0} \\ \mathbf{0} & \mathbf{a}_2 & \cdots & \mathbf{0} \\ \vdots & \vdots & \ddots & \vdots \\ \mathbf{0} & \mathbf{0} & \cdots & \mathbf{a}_{NF} \end{bmatrix}_{3NTF\times 3NF}, \qquad \mathbf{X}_{3D} = \begin{Bmatrix} \mathbf{X}_{3D,1} \\ \mathbf{X}_{3D,2} \\ \vdots \\ \mathbf{X}_{3D,NF} \end{Bmatrix}_{3NF\times 1} \tag{12a–c}$$

in which NTF is the total number of joints at the floors and NF the total number of floors.

Utilizing Equation (11) the static equilibrium can be found as

$$\mathbf{K}_{3D}\mathbf{X}_{3D} = \mathbf{R}_{3D} \tag{13}$$

where

$$\mathbf{K}_{3D} = \mathbf{a}^T\,\mathbf{K}^*_{RR}\,\mathbf{a} \tag{14}$$

$$\mathbf{R}_{3D} = \mathbf{a}^T\,\mathbf{R}^*_{FR} \tag{15}$$

Note that the size of $\mathbf{K}_{3D}$ in Equation (14) is $3NF \times 3NF$, where NF = number of floors, and $\mathbf{X}_{3D}$ is degree of freedom associated with the floor displacements.

For structures subject to earthquake the mass can be lumped at each floor, and comprises 3 elements, i.e., translational mass in 2 directions and rotational mass (mass moment of inertia). The equations of motion for the building system can then be written as

$$\mathbf{M}_{3D}\ddot{\mathbf{X}}_{3D} + \mathbf{C}_{3D}\dot{\mathbf{X}}_{3D} + \mathbf{K}_{3D}\mathbf{X}_{3D} = -\mathbf{M}_{3D}\mathbf{e}_0\ddot{x}_g \tag{16}$$

where vector $\mathbf{e}_0$ in (16) has the form

$$\mathbf{e}_0 = [\mathbf{e}^T_{0,1}, \mathbf{e}^T_{0,2}, \ldots, \mathbf{e}^T_{0,n}]^T, \quad \mathbf{e}_{0,i} = [\cos\theta, \sin\theta, 0]^T,\ i = 1, 2, \ldots, n \tag{17a, b}$$

in which θ the direction angle of earthquake measured from the X-Global Building Co-ordinate.

EFFECT OF PASSIVE MASS DAMPERS

Consider a mass damper that is installed at floor n and attached at a point with arbitrary orientation. Assuming that the damper can only move in one direction, the displacement of the structure at the attachment point in the direction of mass damper can be written as

$$x_0 = \mathbf{a}_0 \mathbf{X}_{3D,n} \tag{18}$$

where

$$\mathbf{a}_0 = [\cos \alpha_D,\ \sin \alpha_D,\ d_0] \tag{19}$$

in which α_D = anti-clockwise angle from the X-Global Building Co-ordinate System to the line of action of the damper's displacement and d_0 = distance from the origin to the line of action of the damper's displacement. The value of d_0 is taken positive when the floor displacement causes positive displacement of the damper and negative otherwise.

The inclusion of the mass damper effect in the equations of motion can be obtained using the Hamilton's principle [24, 25] and defining a kinetic energy and potential energy as

$$T = \tfrac{1}{2}\, \dot{\mathbf{X}}_{a3D}^{T} \mathbf{M}_{3D} \dot{\mathbf{X}}_{a3D} + \tfrac{1}{2} m_d \dot{x}_{da}^2 \tag{20}$$

$$V = \tfrac{1}{2}\, \mathbf{X}_{3D}^{T} \mathbf{K}_{3D} \mathbf{X}_{3D} + \tfrac{1}{2} k_d (x_d - x_0)^2 \tag{21}$$

The variation of work done by the non-conservative force is

$$\delta W_{nc} = \mathbf{f}_{3D}\, \delta \mathbf{X}_{3D} + f_d\, \delta x_d - \mathbf{C}_{3D} \dot{\mathbf{X}}_{3D}\, \delta \mathbf{X}_{3D} - c_d (\dot{x}_d - \dot{x}_0)\, \delta (x_d - x_0) \tag{22}$$

In Equations (20)–(22) m_d, c_d, k_d are the mass, damping and stiffness of the damper, respectively; x_{da} is the absolute displacement of the damper, x_d the relative displacement of the damper, $\mathbf{X}_{a3D}$ the vector of absolute displacement of the structure, $\mathbf{f}_{3D}$ the external load vector in the structure and f_d the external load at mass damper and δ stands for variation.

By defining the Lagrangian $L = T - V$ and applying the Hamilton's principle [24, 25]

$$\int_{t1}^{t2} (\delta L + \delta W_{nc})\, \mathrm{d}t = 0 \tag{23}$$

following integration by parts, the equations of motion can be obtained finally as

$$\mathbf{M}_s \ddot{\mathbf{X}}_s + \mathbf{C}_s \dot{\mathbf{X}}_s + \mathbf{K}_s \mathbf{X}_s = \mathbf{F}_s + \mathbf{e}\, \ddot{x}_g \tag{24}$$

where

$$\mathbf{M}_s = \begin{bmatrix} \mathbf{M}_1 & \mathbf{0} & \cdots & \mathbf{0} & \mathbf{0} \\ \mathbf{0} & \mathbf{M}_2 & \cdots & \mathbf{0} & \mathbf{0} \\ \vdots & \vdots & \ddots & \vdots & \vdots \\ & & & \mathbf{M}_n & \mathbf{0} \\ \mathbf{0} & \mathbf{0} & \cdots & \mathbf{0} & m_d \end{bmatrix}_{(N+1)\times(N+1)}, \quad \mathbf{K}_s = \hat{\mathbf{K}}_{3D} + \hat{\mathbf{K}}_D,$$

$$\mathbf{F}_s = \begin{Bmatrix} \mathbf{f}_{3D} \\ f_d \end{Bmatrix}, \quad \mathbf{e} = -\mathbf{M}_s \hat{\mathbf{e}}_0, \qquad \mathbf{X}_s = [\mathbf{X}_{3D}^{T},\ x_d]^{T} \tag{25a–d}$$

where $\hat{\mathbf{K}}_{3D} = (N+1)\times(N+1)$ stiffness matrix from the contribution of $\mathbf{K}_{3D}$ into the new stiffness matrix, $\hat{\mathbf{K}}_D$ = contribution of mass damper into the new stiffness matrix that has the form

$$\hat{\mathbf{K}}_D = \begin{bmatrix} \mathbf{O}_{[(N+1)-4]\times[(N+1)-4]} & \mathbf{O}_{[(N+1)-4]\times 4} \\ \mathbf{0}_{4\times[(N+1)-4]} & \mathbf{K}_{D\,4\times 4} \end{bmatrix} \tag{26}$$

$$\mathbf{K}_D = \begin{bmatrix} \mathbf{a}_0^T k_d \mathbf{a}_0 & -\mathbf{a}_0^T k_d \\ -k_d \mathbf{a}_0 & k_d \end{bmatrix}_{4\times 4} \tag{27}$$

where N is the total degrees of freedom of the building before incorporating the mass damper. Note that the stiffness matrix due to the contribution of mass damper has the form as in Equation (26) with the assumption that the mass damper is installed at the top floor. If the mass damper is installed at any other floor: $\mathbf{K}_D$ in Equation (27) can be assembled according to the destination vector following the procedure in the standard stiffness matrix method.

The damping contribution of the damper can be performed in a similar way as in the stiffness contribution by replacing the stiffness parameters with the damping parameters. Note that, although the derivation of the equations is performed for one damper only, a similar procedure can be performed when more than one damper is installed at the building.

EFFECT OF ACTIVE CONTROL

When the control force is inserted between the mass damper and the reaction wall the equations of motion can be obtained similarly. In this case the variation due to non-conservative forces in Equation (22) now includes the effect of control force to the system

$$\delta W_{nc} = \mathbf{f}_{3D}\delta\mathbf{X}_{3D} + f_d\delta x_d - u\delta x_0 + u\delta x_d - \mathbf{C}_{3D}\dot{\mathbf{X}}_{3D}\delta\mathbf{X}_{3D} - c_d(\dot{x}_d - \dot{x}_0)\,\delta(x_d - x_0) \tag{28}$$

where u is the control force and x_0 the relative displacement of the structure at the location of mass damper. By utilizing the Hamilton's principle as in the passive control, the equations of motion now can be written as

$$\mathbf{M}_s\ddot{\mathbf{X}}_s + \mathbf{C}_s\dot{\mathbf{X}}_s + \mathbf{K}_s\mathbf{X}_s = \mathbf{F}_s + \mathbf{b}\mathbf{u} + \mathbf{e}\ddot{x}_g \tag{29}$$

where

$$\mathbf{b} = \begin{Bmatrix} \mathbf{0} \\ -\mathbf{a}_0^T \\ 1 \end{Bmatrix}, \quad \mathbf{u} = u. \tag{30a,b}$$

When an active bracing, instead of active mass dampers, is installed at the first storey of the original structure, the variation due to the non-conservative forces is similar to Equation (28) except that the second, third and sixth terms vanish such that

$$\delta W_{nc} = \mathbf{f}_{3D}\delta\mathbf{X}_{3D} + u\delta x_0 - \mathbf{C}_{3D}\dot{\mathbf{X}}_{3D}\delta\mathbf{X}_{3D} \tag{31}$$

in which x_0 is the relative displacement of the structure in the horizontal direction of the control force at the actuator location. The equation of motion is the same as in Equation (29), but with the

size of the matrices now is related to the original degree of freedom of the structure. In this case, the control force location matrix can be written as

$$\mathbf{b} = \begin{Bmatrix} \mathbf{a}_0^{\mathrm{T}} \\ \mathbf{0} \end{Bmatrix} \tag{32}$$

When more than one active force is installed, the control force location matrix can be modified accordingly.

Several subprograms have been developed in MATLAB [26] to perform the structural analysis. The reason to use MATLAB is that it is now widely used especially in control engineering. In that case the developed program can be interconnected with other toolbox in MATLAB.

STATE EQUATIONS AND GENERAL OUTPUT FEEDBACK

The equations of motion of Equation (29) with the absence of the external load can be written as

$$\dot{\mathbf{Z}} = \mathbf{A}\mathbf{Z} + \mathbf{B}\mathbf{u} + \mathbf{E}w \tag{33}$$

where

$$\mathbf{Z} = [\mathbf{X}_{\mathrm{s}}^{\mathrm{T}} \ \dot{\mathbf{X}}_{\mathrm{s}}^{\mathrm{T}}]^{\mathrm{T}}, \quad \mathbf{A} = \begin{bmatrix} \mathbf{0} & \mathbf{I} \\ -\mathbf{M}_{\mathrm{s}}^{-1}\mathbf{K}_{\mathrm{s}} & -\mathbf{M}_{\mathrm{s}}^{-1}\mathbf{C}_{\mathrm{s}} \end{bmatrix}, \quad \mathbf{B} = \begin{bmatrix} 0 \\ \mathbf{M}_{\mathrm{s}}^{-1}\mathbf{b} \end{bmatrix}, \quad \mathbf{E} = \begin{Bmatrix} \mathbf{0} \\ \mathbf{M}_{\mathrm{s}}^{-1}\mathbf{e} \end{Bmatrix}, \ w = \ddot{x}_g \tag{34a–e}$$

Suppose the control force $\mathbf{u}$ is the regulated based on the measurement of the displacement, velocity and absolute acceleration of the structure such that

$$\mathbf{u} = -\mathbf{G}_{\mathrm{d}}\mathbf{C}_{\mathrm{yd}}\mathbf{X}_{\mathrm{s}} - \mathbf{G}_{\mathrm{v}}\mathbf{C}_{\mathrm{yv}}\dot{\mathbf{X}}_{\mathrm{s}} - \mathbf{G}_{\mathrm{a}}\mathbf{C}_{\mathrm{ya}}\ddot{\mathbf{X}}_{\mathrm{sa}} \tag{35}$$

where $\mathbf{G}_{\mathrm{d}}$, $\mathbf{G}_{\mathrm{v}}$ and $\mathbf{G}_{\mathrm{a}}$ are displacement, velocity and absolute acceleration gains, respectively; $\mathbf{C}_{\mathrm{yd}}$, $\mathbf{C}_{\mathrm{yv}}$ and $\mathbf{C}_{\mathrm{ya}}$ are observation matrices related to displacement, velocity and absolute measurements, respectively and $\ddot{\mathbf{X}}_{\mathrm{sa}}$ = absolute acceleration of the structure. By substituting the control force $\mathbf{u}$ into the equations of motion, the absolute acceleration of the structure can be written as

$$\ddot{\mathbf{X}}_{\mathrm{sa}} = \mathbf{C}_{\mathrm{sa}}\mathbf{Z} \tag{36}$$

where

$$\mathbf{C}_{\mathrm{sa}} = \lfloor -\mathbf{M}_{\mathrm{cl}}^{-1}\mathbf{K}_{\mathrm{cl}} \quad -\mathbf{M}_{\mathrm{cl}}^{-1}\mathbf{C}_{\mathrm{cl}} \rfloor, \quad \mathbf{M}_{\mathrm{cl}} = \mathbf{M}_{\mathrm{s}} + \mathbf{b}\,\mathbf{G}_{\mathrm{a}}\,\mathbf{C}_{\mathrm{ya}},$$
$$\mathbf{C}_{\mathrm{cl}} = \mathbf{C}_{\mathrm{s}} + \mathbf{b}\,\mathbf{G}_{\mathrm{v}}\,\mathbf{C}_{\mathrm{yv}}, \quad \mathbf{K}_{\mathrm{cl}} = \mathbf{K}_{\mathrm{s}} + \mathbf{b}\,\mathbf{G}_{\mathrm{d}}\,\mathbf{C}_{\mathrm{yd}} \tag{37a–d}$$

Utilizing Equations (36) and (37) the control force can be written as

$$\mathbf{u} = -\mathbf{G}\mathbf{y} \tag{38}$$

where $\mathbf{G}$ is the gain matrix and $\mathbf{y}$ the measurement of the structural response which can be obtained as

$$\mathbf{y} = \begin{bmatrix} \mathbf{C}_{yd} & \mathbf{0} \\ \mathbf{0} & \mathbf{C}_{yv} \\ \mathbf{C}_{ya} & \mathbf{C}_{sa} \end{bmatrix} \mathbf{Z} = \mathbf{C}_y \mathbf{Z} \tag{39}$$

Note that Equation (39) is a general form of measurement output that contains displacement and velocity as well as absolute acceleration of the structure.

By substituting the control force in Equation (38) into Equation (33) the closed loop system can be obtained as

$$\dot{\mathbf{Z}} = \mathbf{A}_{cl}\mathbf{Z} + \mathbf{E}\mathbf{w} \tag{40}$$

where

$$\mathbf{A}_{cl} = \mathbf{A} - \mathbf{B}\mathbf{G}\mathbf{C}_y \tag{41}$$

The regulated (controlled) output $\mathbf{z}$, as the response that we wish to minimize, can be represented in a similar way as in the measurement output as

$$\mathbf{z} = \mathbf{C}_z \mathbf{Z} \tag{42}$$

where $\mathbf{C}_z$ is the regulation matrix.

OPTIMAL DESIGN

Performance indices

Several performance indices have been proposed in the control theory as criteria of the optimality. At the beginning of the modern control technique, the Linear Quadratic Regulator (LQR) was widely used as the replacement of the frequency domain techniques. However, LQR controller needs a full state, i.e., all displacements and velocities, for the feedback. As LQR controller is not practical to be used, recently the H_2, H_∞ and L_1 norms, which are employed in this paper, have also been proposed. In these types of performance objective, the norms of transfer functions from external disturbance to the regulated output should be minimum.

Consider the state space equation

$$\dot{\mathbf{Z}} = \tilde{\mathbf{A}}\mathbf{Z} + \mathbf{E}\mathbf{w} \tag{43}$$

Equation (43) can be considered as an active control system when $\tilde{\mathbf{A}} = \mathbf{A}_{cl}$ or passive control when $\tilde{\mathbf{A}} = \mathbf{A}$.

In H_2 optimization, the H_2 norm is taken as the performance measure of the optimality. For the system in Equation (43) with the regulated output in Equation (42) the H_2 norm transfer functions from the external disturbance $\mathbf{w}$ to the regulated output $\mathbf{z}$ can be computed as [27]

$$\| T_{zw} \|_2 = [\mathrm{tr}(\mathbf{C}_z \mathbf{L}_c \mathbf{C}_z^T)]^{1/2} = [\mathrm{tr}(\mathbf{E}^T \mathbf{L}_0 \mathbf{E})]^{1/2} \tag{44}$$

where $\mathbf{L}_c$ and $\mathbf{L}_0$ are controllability and observability Gramians which can be obtained from the solution of the Lyapunov equations

$$\tilde{\mathbf{A}}\mathbf{L}_c + \mathbf{L}_c\tilde{\mathbf{A}}^T + \mathbf{E}\mathbf{E}^T = \mathbf{0} \text{ or } \tilde{\mathbf{A}}^T\mathbf{L}_0 + \mathbf{L}_0\tilde{\mathbf{A}} + \mathbf{C}_z^T\mathbf{C}_z = \mathbf{0} \tag{45a,b}$$

In H_∞ optimization, the H_∞ norm transfer functions from the external disturbance to the regulated output is chosen as the performance index and may be calculated by first defining the Hamiltonian matrix

$$\mathbf{H} = \begin{bmatrix} \tilde{\mathbf{A}} & \gamma^2 \mathbf{E}\mathbf{E}^{\mathrm{T}} \\ -\mathbf{C}_z \mathbf{C}_z^{\mathrm{T}} & -\tilde{\mathbf{A}}^{\mathrm{T}} \end{bmatrix} \tag{46}$$

The H_∞ norm is computed as follows [27]: (i) Choose a positive number γ, (ii) calculate the eigenvalue of $\mathbf{H}$, (iii) if $\mathbf{H}$ has no imaginary eigenvalues reduce γ, otherwise increase γ. The final value of γ represents the H_∞ norm of the transfer function from external disturbance to the regulated output.

In L_1 norm optimization considered in this paper, the performance index to be minimized is the L_1 norm bound as discussed in Haddad and Chellaboina [28] as follows:

$$\| T_{zw} \|_1 \leqslant [\sigma_{\max} (\mathbf{C}_z \ \mathbf{Q} \ \mathbf{C}_z^{\mathrm{T}})]^{1/2} \tag{47}$$

where $\mathbf{Q}$ can be obtained from the solution of

$$\tilde{\mathbf{A}}\mathbf{Q} + \mathbf{Q}\tilde{\mathbf{A}}^{\mathrm{T}} + \alpha \mathbf{Q} + \frac{1}{\alpha} \mathbf{E} \ \mathbf{E}^{\mathrm{T}} = \mathbf{0} \tag{48}$$

for $\alpha > 0$.

It is also common to combine the objective by minimizing a certain norm with the constraints of other norms. In addition, it is also possible to simultaneously optimize the passive and active parameters of the system. In this case, the system matrix $\tilde{\mathbf{A}}$ contains structural parameters of the passive devices as well as controlled gains.

Once the performance indices defined above are chosen the optimization procedure can be performed. The computation of transfer function norms defined above is carried out using the functions *norm* and *lyap* within the MATLAB Control System Toolbox. To obtain design variables that minimize the performance index several algorithms can be utilized. In this paper, the genetic based optimizer is used.

Genetic algorithm for structural control

A genetic algorithm (GA) [29] that has been successfully applied in many optimization areas [30, 31] is used in this paper as a function optimizer. GA is a search algorithm that starts the solution from many different starting points. Candidates of the solution are initially generated randomly as the initial population of design variables. These candidates of the solution are experiencing genetic changes following Darwinian's natural selection. Individuals that have high fitness, which can be measured according to the defined objective function, have a larger probability to be passed into the next generation than the low fitness individuals. The selected individuals are then changing the chromosomal structures through cross-over and mutation. The process of selection, cross-over and mutation are repeatedly done generation after generation. At the final generation, the best individual is taken as the optimum design.

At the early stage of the GA development, the individuals are represented by binary strings that contain 0 and 1. This string is a mapping of the real value of design variables based on the upper and lower bound values of design variables. Therefore, the length of the bit string depends on the upper and lower bound values as well as the precision requirement of the design variable. Recently the real coding GA has also been used and successfully implemented for the function

optimizer as in the binary coding. In real coding the individual is represented by a real vector of design variables.

The fitness of each individual can be obtained from the defined objective function. Note that in GA, the problem is to maximize the fitness and therefore, the fitness function should have a positive value. In this case, the objective function should be modified such that it always results in a positive number as:

$$F_t = \alpha_f / J \tag{49}$$

where J is the objective function and α_f, a scalar to scale the fitness value.

When there are constraints, the penalty function can be applied to the objective function. If there are r constraints that should be satisfied by J_i to a certain level ct_i as

$$J_i \leqslant ct_i, \quad i = 1, 2, \ldots, r \tag{50}$$

then for every violation of the constraints, the fitness may be modified as

$$F_{t,\text{new}} = p_i \, F_{t,\text{old}}. \tag{51}$$

where p_i is the penalty to the violated individual to each constraint. The penalty p_i may be taken as $\exp(-J_i/ct_i)$ which represents how far the degree of satisfaction is. In active control, it is also possible that the feedback loop causes instability to the structure. To prevent this condition, the fitness of the individual that has positive real part of eigenvalues (after the introduction of the active control) is assigned to have a zero fitness or a very small fitness value.

After computing the fitness of the individuals, the selection procedure can be performed to locate individuals in the mating pool. The selection procedure employed in this paper is the roulette wheel selection procedure [30]. Detail explanation of this selection procedure can be found in Reference [30].

The selected individuals in the mating pool are then interchanging the chromosomal information through cross-over. Two parents are selected for cross-over and the information contained within individuals is interchanged. For binary coding, the cross-over can be performed such that, for one point cross-over, the first offspring receives the chromosome from the first parent up to the cross-over site plus the chromosome of second parent after the cross-over site; while the second offspring receives the first part chromosome from the second parent up to the cross-over site plus the chromosome of the first parent after the cross-over site. For real coding, there are several modified cross-over operators that can be performed such as arithmetical cross-over, guaranteed average cross-over and heuristic crossover [30, 31]. One type of cross-over that has the capability to explore the unknown domain of the search space may be performed as

$$G_1' = \rho(G_1 - G_2) + G_1 \tag{52a}$$

and

$$G_2' = \rho(G_2 - G_1) + G_2 \tag{52b}$$

This types of cross-over is suitable to be used in active control design, since the domain of the controller gains is usually unknown of difficult to predict. Although it is possible to define the domain of the search of the controller gain to lay in the range of a stabilizing gain by using Routh–Hurwitz criterion, for MIMO (multi-input multi-output) system this strategy is very tedious. Therefore, the cross-over that can explore a larger domain is expected and appropriate for the application in the active control system.

After cross-over, individuals undergo mutation. For binary coding, the mutation is performed by changing the bits from 0 to 1 and 1 to 0. For real coding, the mutation may be performed to the original chromosome

$$G = [g_1, g_2, \ldots, g_i, \ldots, g_n]$$

with the ith design variable is chosen for mutation, the new chromosome will be

$$G' = \lfloor g_1, g_2, \ldots, g_i', \ldots, g_n \rfloor$$

where

$$g_i' = \rho a g_i \tag{53}$$

in which ρ is the random number between 0 and 1 and $a > 1$. Note that several mutation procedures for real coded GA may be performed [31, 32].

The selection, cross-over, and mutation process is performed generation after generation. The best individual at the final generation is chosen as the optimum design. In this paper the mechanics of standard GA is modified, where after selection, cross-over and mutation, a number of new individuals are inserted in every generation replacing the current individuals in the population randomly. In addition, to ensure that the best individual in each generation is always copied into the next generation, the elitist strategy is also adopted in this paper. The code of GA written in MATLAB has been developed to automate the optimization process.

NUMERICAL EXAMPLE

Control using passive TMDs

A three-dimensional building as shown in Figure 2 is used as an example. The stiffness matrix and mass matrices were obtained according to the procedure discussed above utilizing the developed structural analysis program. The origin of the Global Building Coordinate Systems is assumed at the centre of mass of each floor. The stiffness and the mass matrices are as follows:

$$\begin{aligned}\mathbf{K}_{3D} = 1 \times 10^5\ [&0.250438\ \ 0.000054\ \ 0.050552\ \ -0.121076\ \ -0.000077\ \ -0.023722;\ 0.000054\\ &0.250438\ \ 0.050552\ \ -0.000077\ \ -0121076\ \ -0.023722;\ 0.050552\ \ 0.050552\\ &8.063055\ \ -0.023720\ \ -0.023720\ \ -3.913086;\ \ -0.121076\ \ -0.000077\\ &-0.023720\ \ 0.113590\ \ 0.000122\ \ 0.021139;\ \ -0.000077\ \ -0.121076\\ &-0.023720\ \ 0.000122\ \ 0.113590\ \ 0.021139;\ \ -0.023722\ \ -0.023722\\ &-3.913086\ \ 0.021139\ \ 0.021139\ \ 3.692753]\end{aligned}$$

and

$$\mathbf{M}_{3D} = \text{diag}\ [77.16, 77.16, 1178.835, 67.46, 67.46, 1030.64],$$

respectively. Note that the stiffness matrix above is written in the MATLAB type, and diag in mass matrix stands for diagonal.

With the stiffness and mass matrices defined above, the natural frequencies of the structure are 7.82, 7.83, 11.44, 20.73, 20.77 and 30.23 rad/s. The damping matrix is assumed to be proportional

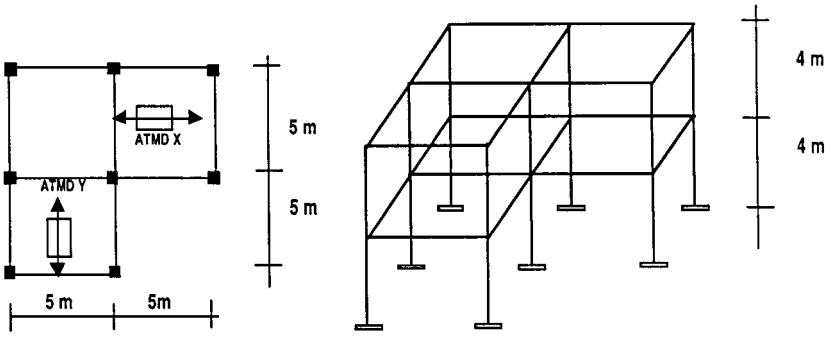

Figure 2. Example building.

to the stiffness matrix, $\mathbf{C}_{3D} = \beta \mathbf{K}_{3D}$. Assuming that the structure has 1.5 per cent of critical damping at the first mode, the coefficient β is found to be 3.84×10^{-3}.

Two mass dampers are attached on the top floor to control the structure's vibration. The first damper is installed in the x-direction and the second one in the y-direction. The total mass of the dampers is taken as 1.5 per cent of the total mass of the building which results in $m_{d1} = m_{d2} = 1.08$ t. It is assumed the mass of the building does not change due to the installation of the mass dampers.

By the addition of mass dampers, total degree of freedom of the structure becomes 8, with the 7th and 8th degrees of freedom denoting the displacement of the x and y dampers with respect to the ground, respectively. The stiffness matrix now can be obtained according to the method discussed above, where the transformation matrix for the x and y mass dampers are $\mathbf{a}_{0x} = [1\ \ 0, -1.67]$, and $\mathbf{a}_{0y} = [0,\ 1,\ -1.67]$, respectively; and the destination vectors of the x and y dampers are $\mathbf{id}_x = [4,\ \ 5,\ \ 6,\ \ 7]$ and $\mathbf{id}_y = [4,\ \ 5,\ \ 6,\ \ 8]$, respectively.

To optimize the TMD parameters, the GA is used as an optimizer where the H_2 based norm is taken as the objective function. Due to the geometry of the structure the TMD parameters are taken to be the same properties such that $k_{dx} = k_{dy}$ and $c_{dx} = c_{dy}$. By using these properties, only one direction of earthquake is considered to capture the behaviour of the structure due to bi-directional earthquake.

Several cases of optimization are conducted, by modifying the performance indices and regulated outputs. The regulation matrices have been chosen as follows: (i) $\mathbf{C}_z = [\mathbf{I}_{6\times 6},\ \mathbf{0}_{6\times 10}]$, (ii) $\mathbf{C}_{z1} = [\mathbf{0}_{1\times 3},\ \mathbf{1},\ \mathbf{0}_{1\times 12}]$, (iii) $\mathbf{C}_{z2} = [\mathbf{0}_{1\times 4},\ \mathbf{1},\ \mathbf{0}_{1\times 11}]$, (iv) $\mathbf{C}_{z3} = [\mathbf{0}_{1\times 5},\ \mathbf{1},\ \mathbf{0}_{1\times 10}]$, which represent minimization of (i) displacement, (ii) x-displacement of the second floor, (iii) y-displacement of second floor, (iv) rotation of the second floor, respectively. The H_2 norm of the transfer function from the external disturbance to each regulated output defined above are denoted as J, J_1, J_2 and J_3, respectively.

In addition to the regulated outputs above, several cases are considered as follows:

a. Objective function is J without constraint,
b. Objective function is J with constraint $J_i\,(i = 1, 2, 3)$ less than $0.7\,H_{2i}$, where $H_{2i} = H_2$ norm transfer function from external disturbance to the regulated output, where the regulated output is the same as in J_i for the uncontrolled case (without passive mass dampers),

Table I. Optimization results of passive mass dampers.

	Case *a*	Case *b*	Case *c*	Case *d*
k_d (kN/m)	64.9	60.61	53.78	55.48
c_d (kN s/m)	0.9156	0.9156	0.7325	0.8546
J_1/H_{21} (%)	62.66	64.09	73.93	70.47
J_2/H_{22} (%)	50.29	34.43	22.95	24.59
J_3/H_{23} (%)	75.44	69.23	69.23	65.38

Table II. Peak responses for several cases of passive TMD.

	Uncontrolled	Case *a*	Case *b*	Case *c*	Case *d*
		El Centro 1940 *NS in x direction*			
r_{x2} (m)	0.1409	0.1210	0.1213	0.1216	0.1216
r_{y2} (m)	0.0023	0.0025	0.0019	0.001	0.0012
$r_{\theta 2}$ (rad)	0.0022	0.0022	0.0020	0.0018	0.0022
r_{x1} (m)	0.0836	0.0692	0.0681	0.0684	0.0684
r_{y1} (m)	0.0014	0.0014	0.0011	0.0005	0.0006
$r_{\theta 1}$ (rad)	0.0014	0.0013	0.0012	0.0010	0.0011
		Northridge 1994 *in x direction*			
r_{x2} (m)	0.2477	0.2406	0.2410	0.2417	0.2415
r_{y2} (m)	0.0046	0.0023	0.0018	0.0013	0.0013
$r_{\theta 2}$ (rad)	0.0030	0.0030	0.0030	0.0029	0.0030
r_{x1} (m)	0.1295	0.1256	0.1258	0.1264	0.1262
r_{y1} (m)	0.0027	0.0014	0.001	0.0007	0.0008
$r_{\theta 1}$ (rad)	0.0019	0.0019	0.0019	0.0018	0.0019

c. Objective function is $J_1 \times J_2 \times J_3$ without constraint,
d. Objective function is $J_1 \times J_2 \times J_3$ with constraint the same as in the case *b*.

The binary coded GA has been used to obtain the optimum parameters of k_d and c_d. The resulting k_d and c_d as well as the ratio of the defined norm in the objective function are presented in Table I. Note that in case *d* the constraint is slightly violated, although the difference is very small. Peak responses of the structure subjected to El Centro 1940 NS and Northridge excitations are presented in Table II while the time history response of the structure for case *d* is shown in Figure 3.

Control using active tuned mass dampers

To increase the capability of the passive control, an actuator is installed in each tuned mass damper to drive the control force to the structure. The damper parameters taken here are from

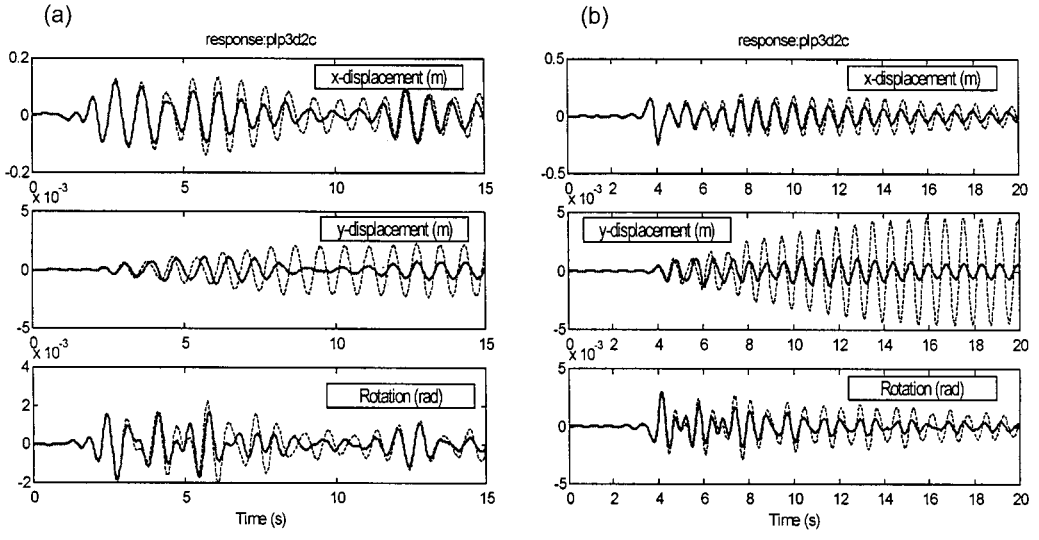

Figure 3. Displacement of 2nd floor due to (a) El Centro 1940 NS, (b) Northridge 1994 NS excitations applied in x-direction, passive TMDs case d: (- - - -) uncontrolled, (——) passive control.

case c of the passive optimization discussed above. The equations of motion can be written as in Equation (33) where

$$\mathbf{B} = \begin{bmatrix} \mathbf{0}_{8\times 2} \\ \mathbf{M}_s^{-1}\mathbf{b} \end{bmatrix}, \quad \mathbf{b} = \begin{bmatrix} \mathbf{0} & \mathbf{0} \\ -\mathbf{a}_{ox}^{T} & -\mathbf{a}_{oy}^{T} \\ 1 & 0 \\ 0 & 1 \end{bmatrix}$$

Note that if needed, it is possible to do the optimization of passive and active control simultaneously.

Similar to the passive control, various possible performance indices may be chosen as the optimality criteria in the active control optimization. Suppose the objective is to minimize the H_2 norm transfer function from the external disturbance to the x-displacement of the second floor due to the x earthquake. Since we only define a simple objective, while we want to minimize the response in all directions due to the x or y earthquake excitation, we impose other objective using the constraints. The constraints are chosen such that the H_2 norm of transfer function from either the x and y disturbance to the 2nd floor displacement (x and y displacements and rotation) should be less than 0.85 of those norms of the passive control case.

The feedback are taken as absolute accelerations of the second floor in the x and y directions, absolute accelerations of TMDs, velocities of TMDs and displacement of the second floor in x and y directions. In this case the gain matrices are

$$\mathbf{G}_a = \begin{bmatrix} 0 & 0 & 0 & G_{a1} & G_{a2} & 0 & G_{a3} & G_{a4} \\ 0 & 0 & 0 & G_{a5} & G_{a6} & 0 & G_{a7} & G_{a8} \end{bmatrix}$$

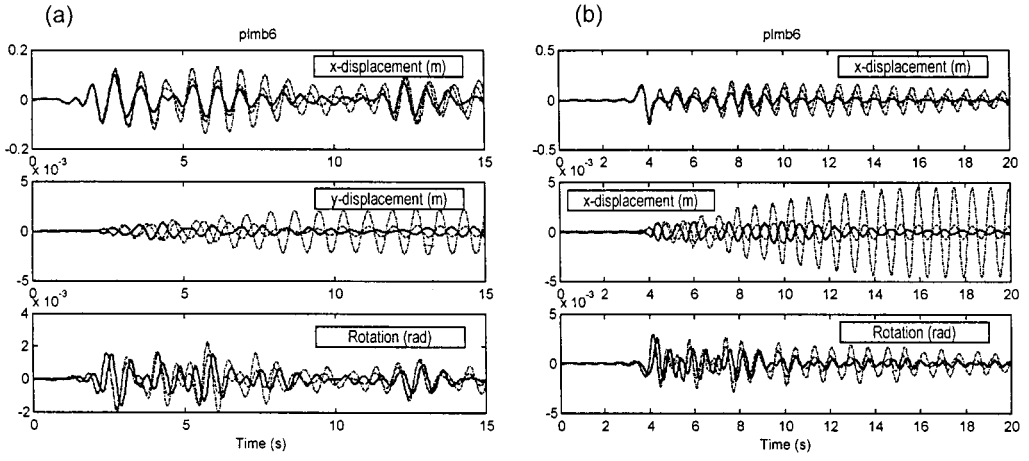

Figure 4. Displacement of 2nd floor due to (a) El Centro 1940 NS, (b) Northridge 1994 NS excitations applied in x-direction, case ATMD: (–·–·–·) uncontrolled, (- - - -) passive TMDs' (——) active TMDs.

$$\mathbf{G}_{\mathrm{v}} = \begin{bmatrix} 0 & 0 & 0 & 0 & 0 & 0 & G_{v1} & G_{v2} \\ 0 & 0 & 0 & 0 & 0 & 0 & G_{v3} & G_{v4} \end{bmatrix}$$

$$\mathbf{G}_{\mathrm{d}} = \begin{bmatrix} 0 & 0 & 0 & G_{d1} & G_{d2} & 0 & 0 & 0 \\ 0 & 0 & 0 & G_{d3} & G_{d4} & 0 & 0 & 0 \end{bmatrix}$$

Note that due to the geometry and properties of the structural system including TMDs we may take $G_{a5} = G_{a2}$, $G_{a6} = G_{a1}$, $G_{a7} = G_{a4}$, $G_{a8} = G_{a3}$, $G_{v3} = G_{v2}$, $G_{v4} = G_{v1}$, $G_{d3} = G_{d2}$ and $G_{d4} = G_{d1}$ such that we impose the structure to resist the earthquake from x and y directions equally and reduce the design variable from 16 to 8 only.

The real coded GA is used to obtain the controller gains. GA will search such controller gains and locate the most probable gains to meet the objective. It is to be noted that the resulting controller here almost meets the constraints where the ratio of the H_2 norm of active case to passive case for x and y displacements and rotation of the second floor are 0.6459, 0.8649 and 0.8678, respectively. The time history response of the structure due to El-Centro 1940 NS and Northridge 1994 excitations applied in the x direction can be seen in Figure 4 with the maximum control forces are 43.2 and 136.7 kN, respectively. The peak responses are also presented in Table III.

Control using active bracing systems

Active bracing systems are now installed at the first storey without passive and active TMD as can be seen in Figure 5. With this active bracing system the mass, damping and stiffness matrices are assumed to be the same as in uncontrolled case. The matrix $\mathbf{B}$ and control vector $\mathbf{u}$ are

$$\mathbf{B} = \begin{bmatrix} \mathbf{0}_{6\times 4} \\ \mathbf{M}_{\mathrm{s}}^{-1}\mathbf{b} \end{bmatrix}, \quad \mathbf{b} = [\mathbf{b}_1 \quad \mathbf{b}_2 \quad \mathbf{b}_3 \quad \mathbf{b}_4], \quad \mathbf{b}_i = \begin{Bmatrix} \mathbf{a}_i^{\mathrm{T}} \\ \mathbf{0}_{3\times 1} \end{Bmatrix}_{6\times 1}, \; i = 1, 2, 3, 4$$

Table III. Peak responses for various active control systems.

	Uncontrolled	Passive TMD	Active TMD	Active Bracing case *a*	Active Bracing case *b*	Active Bracing case *c*
			El Centro 1940 *NS in x direction*			
r_{x2} (m)	0.1409	0.1216	0.0997	0.0821	0.0927	0.0818
r_{y2} (m)	0.0023	0.0010	0.0009	0.0009	0.0005	0.0006
$r_{\theta 2}$ (rad)	0.0022	0.0018	0.0016	0.0015	0.0016	0.0015
r_{x1} (m)	0.0836	0.0684	0.0589	0.0469	0.0514	0.0468
r_{y1} (m)	0.0014	0.0005	0.0005	0.0009	0.0004	0.0008
$r_{\theta 1}$ (rad)	0.0014	0.0010	0.0009	0.0009	0.0014	0.0009
$u_{\max}$ (kN)	—	—	43.2	123.6	124.8	125.8
			Northridge 1994 *in x direction*			
r_{x2} (m)	0.2477	0.2417	0.2118	0.1778	0.1962	0.1772
r_{y2} (m)	0.0046	0.0013	0.0011	0.0022	0.0009	0.0022
$r_{\theta 2}$ (rad)	0.0030	0.0029	0.0026	0.0022	0.0024	0.0022
r_{x1} (m)	0.1295	0.1264	0.1163	0.0878	0.0961	0.0878
r_{y1} (m)	0.0027	0.0007	0.0008	0.0032	0.0009	0.0031
$r_{\theta 1}$ (rad)	0.0019	0.0018	0.0015	0.0015	0.0016	0.0015
$u_{\max}$ (kN)	—	—	136.7	298.3	299.8	303.5

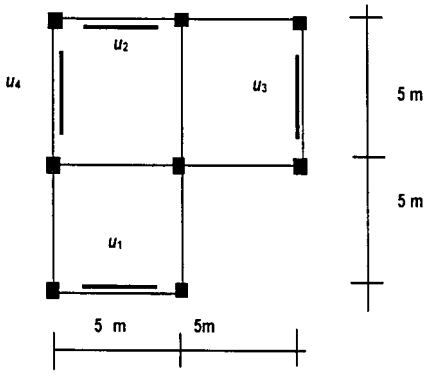

Figure 5. Location of the active bracing.

where the transformation matrix $\mathbf{a}_i$ $(i = 1, 2, 3, 4)$ are $\mathbf{a}_1 = [1, \quad 0, \quad 5.83]$, $\mathbf{a}_2 = [1, \quad 0, \quad -4.17]$, $\mathbf{a}_3 = [0, \quad 1, \quad 5.83]$ and $\mathbf{a}_4 = [0, \quad 1, \quad -4.17]$.

Suppose the velocities of the second floor in the x and y directions are chosen as the feedback. Several performance indices have been defined as follows:

(a) H_2 norm transfer function from the x-direction of earthquake to the x displacement of the second floor, with the constraints are H_2 norm transfer function from the x and y earthquakes to the x and y displacements and rotation of the second floor should be less than 0.5 of those norms of the uncontrolled case.

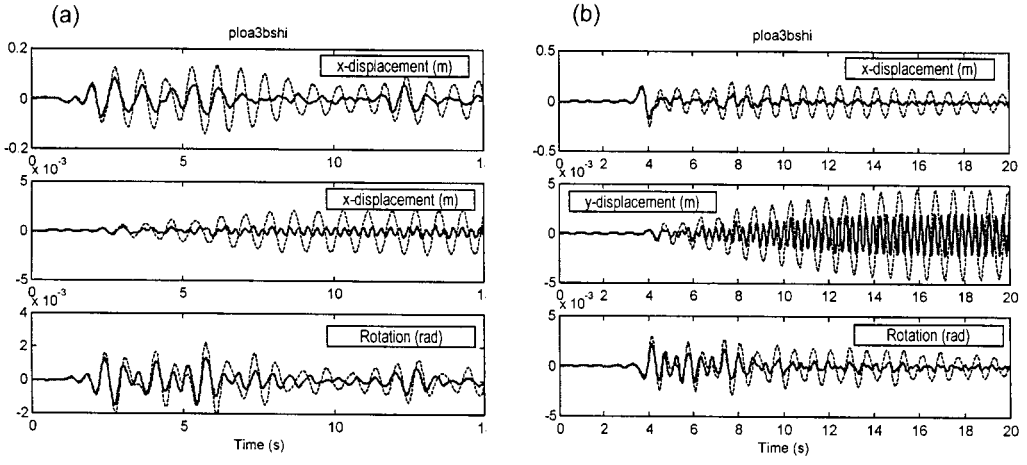

Figure 6. Displacement of 2nd floor due to (a) El Centro 1940 NS, (b) Northridge 1994 NS excitations applied in x-direction, active bracing case c: (- - - -) uncontrolled, (——) active bracing.

(b) $L_{11,x} * L_{12,x} * L_{13,x} * L_{11,y} * L_{12,y} * L_{13,y}$, where $L_{11,x}$, $L_{12,x}$ and $L_{13,x} = L_1$ norm transfer function from the x-direction of earthquake to the displacement of the second floor of the x and y displacements and rotation, respectively, with the constraints are the same as above.

(c) H_∞ norm transfer function from the x-direction of earthquake to the x displacement of the second floor with constraints are the same as in (a).

The ratio of H_2 norm of the active to passive case from the x earthquake to the displacements of the second floor in the x and y directions and rotation, respectively, are: (i) 0.3752, 0.5008 and 0.5118 for case a, (ii) 0.4285, 0.1070 and 0.5546 for case b, and (iii) 0.3749, 0.5026 and 0.5126 for case c, respectively. The time history response for case C due to El-Centro 1940 NS and Northridge 1994 excitations applied in the x direction are depicted in Figure 6. The peak responses are also presented in Table III.

CONCLUSIONS

Three-dimensional analysis of buildings with passive and active control is discussed in this paper. The building is modelled by assuming the floor as a rigid diaphragm. The inclusion of the passive and active control devices is obtained by using the Hamilton's principle. Both passive and active controls are optimized based on the performance indices used in modern control theory, i.e. H_2, H_∞ and L_1 norms, where the genetic algorithm (GA) is employed to obtain the optimal parameters. Binary and real coded GAs can be used to optimize the defined performance index. Note that the real coded GA is more appropriate to be used in the active control system since it has the capability to explore the unknown domain that is impossible to handle by binary coded

GA. For the active control, the controller used in this paper is a direct (static) output feedback controller where the measurement is directly multiplied by the gain.

REFERENCES

1. Yao JTP. Concept of structural control. *Journal of Structural Division*, ASCE, 1972; **98**(ST7):1567–1574.
2. Chung LL, Reinhorn AM, Song TT. Experiments on active control of seismic structures. *Journal of Engineering Mechanics*, ASCE 1998; **114**(2):241–256.
3. Chang JCH, Soong TT. Structural control using active tuned mass dampers. *Journal of Engineering Mechanical Division*, ASCE 1980; **EM6**(106):1091–1098.
4. Soong TT, Reinhorn AM, Wang YP, Lin RC. Full scale implementation of active control. I: design and simulation. *Journal of Structural Engineering*, ASCE 1992; **117**(11):3516–3536.
5. Makris N, Burton SA, Hill D, Jordon M. Analysis and design of ER damper for seismic protection of structures. *Journal of Engineering Mechanics* ASCE 1996; **122**:1003–1011.
6. Spencer BF, Dyke SJ, Sain MK, Carlson JD. Phenomenological model of a magnetorheological damper. *Journal of Engineering Mechanics*, ASCE 1997; **123**(3):230–238.
7. Samali B, Yang JN, Yeh CT. Control of lateral-torsional motion of wind-excited buildings. *Journal of Engineering Mechanics*, ASCE 1985; 1**11**(6):777–796.
8. Kobori T, Koshika N, Yamada K, Ikeda Y. Seismic response controlled structures with active mass driver system. Part I: design. *Earthquake Engineering and Structural Dynamics* 1991; **20**:135–149.
9. Kobori T, Koshika N, Yamada K, Ikeda Y. Seismic response controlled structures with active mass driver system. Part II: verification. *Earthquake Engineering and Structural Dynamics* 1991; **20**:151–166.
10. Higashino M, Aizawa S. The application of active mass damper system in actual buildings. In *Proceedings of the International Workshop on Structural Control*, Housner GW, Masri SF. (eds.), Los Angeles, CA, 1993; 194–205.
11. Maebayashi K, Tamura K, Shiba K, Ogawa Y, Inada Y. performance of hybrid mass damper system implemented in a tall building. In *Proceedings of the International Workshop on Structural Control*, Housner GW, Masri SF. (eds.), Los Angeles, CA, 1993; 318–328.
12. Fur LS, Yang HTY, Ankiredi S. Vibration control of tall buildings under seismic and wind loads. *Journal of Structural Engineering* 1996; **122**(8):948–957.
13. Kan CL, Chopra AK. Elastic earthquake analysis of torsionally coupled multistorey buildings. *Earthquake Engineering and Structural Dynamics* 1997; **5**:395–412.
14. Loh CH, Lin PY. Kalman filter approach for the control of seismic-induced building vibration using active mass damper systems. *The Structural Design of Tall Buildings* 1977; **6**:209–224.
15. Arfiadi Y, Hadi MNS. On the use of genetic algorithm for optimal control force in active vibration control. *Proceedings of the Australasian Conference in Structural Optimisation*, Sydney, Australia, 1998; 207–214.
16. Hadi MNS, Arfiadi Y. Optimum design of absorber for MDOF structures. *Journal of Structural Engineering* ASCE 1998; **124**(11):1272–1280.
17. Weaver Jr. W, Nelson MF. Three-dimensional analysis of tier buildings. *Journal of Structural Division*, ASCE 1966; **92**(ST6):383–404.
18. Weaver Jr. W, Nelson MF, Maning TA. Dynamics of tier buildings. *Journal of Engineering Mechanics Division*, ASCE 1968; **94**(EM6):1455–1474.
19. Wilson EL, Holling JP, Dovey HH. *Three dimensional analysis of building systems* (*extended version*). Report no EERC 75-13, Earthquake Engineering Research Center, College of Engineering, University of California, Berkeley, California, 1975.
20. Wilson EL, Dovey HH, Habibullah A. *Three dimensional analysis of building systems TABS 80 volume I theoretical manual*. Computer/Structures International, 1980.
21. Humar JL, Khandoker JU. A computer program for three dimensional analysis of buildings. *Computer and Structures* 1980; **11**:369–387.
22. Thambiratnam DP, Irvine HM. Microcomputer analysis of torsionally coupled multistorey building — I shear beam model. *Computer and Structures*, 1989; **32**(5):1175–1182.
23. Beaufait FW, Rowan WH, Hoadley PG, Hacket RMM. *Computer Methods of Structural Analysis*. Prentice-Hall: Englewood Cliffs, NJ. 1970.
24. Clough RW, Penzien J. *Dynamics of Structures*. McGraw-Hill, Kogakusha: Tokyo, 1975.
25. Meirovitch L. *Dynamics and Control of Structures*. Wiley: Singapore, 1990.
26. The Math Work Inc. *MATLAB*, 1997.
27. Doyle JC, Glover K, Khargonekar P, Francis B. State space solutions to standard H_2 and H_∞ control problems. *IEEE Transaction on Automatic Control*. 1989; **34**:831–847.

28. Haddad WM, Chellaboina VS. Mixed norm H_2/L_1 controller synthesis via fixed-order dynamic compensation: a Riccati equation approach. *International Journal of Control* 1998; **71**(1):35–59.
29. Holland J. *Adaptation in Natural and Artificial Systems*. MIT Press: Cambridge, MA, 1994.
30. Goldberg DE. *Genetic Algorithm in Search, Optimization and Machine Learning*. Addison-Wesley Publishing Co: Reading, MA, 1989.
31. Michalewicz Z. *Genetic Algorithms + Data Structures = Evolution Programs*. Springer: Berlin, 1996.
32. Herrera F, Lozano M, Verdegay JL. Tackling real-roded genetic algorithms: operator and tools for behavioural analysis. *Artificial Intelligence Review* 1998; (12):265–319.

